JOURNAL OF BACTERIOLOGY, Dec. 2004, p. 8254–8266 Vol. 186, No. 24
0021-9193/04/$08.00+0 DOI: 10.1128/JB.186.24.8254–8266.2004
Copyright © 2004, American Society for Microbiology. All Rights Reserved.

Dynamics and Control of Biofilms of the Oligotrophic Bacterium *Caulobacter crescentus*

Plamena Entcheva-Dimitrov[1] and Alfred M. Spormann[1,2,3]*

Departments of Civil and Environmental Engineering,[1] Biological Sciences,[2] and Geological and Environmental Sciences,[3] Stanford University, Stanford, California

Received 30 June 2004/Accepted 3 September 2004

Caulobacter crescentus **is an oligotrophic α-proteobacterium with a complex cell cycle involving sessile-stalked and piliated, flagellated swarmer cells. Because the natural lifestyle of *C. crescentus* intrinsically involves a surface-associated, sessile state, we investigated the dynamics and control of *C. crescentus* biofilms developing on glass surfaces in a hydrodynamic system. In contrast to biofilms of the well-studied *Pseudomonas aeruginosa*, *Escherichia coli*, and *Vibrio cholerae*, *C. crescentus* CB15 cells form biphasic biofilms, consisting predominantly of a cell monolayer biofilm and a biofilm containing densely packed, mushroom-shaped structures. Based on comparisons between the *C. crescentus* strain CB15 wild type and its holdfast (*hfsA*; ΔCC0095), pili (Δ*pilA-cpaF*::Ω*aac3*), motility (*motA*), flagellum (*flgH*) mutants, and a double mutant lacking holdfast and flagellum (*hfsA*; *flgH*), a model for biofilm formation in *C. crescentus* is proposed. For both biofilm forms, the holdfast structure at the tip of a stalked cell is crucial for mediating the initial attachment. Swimming motility by means of the single polar flagellum enhances initial attachment and enables progeny swarmer cells to escape from the monolayer biofilm. The flagellum structure also contributes to maintaining the mushroom structure. Type IV pili enhance but are not absolutely required for the initial adhesion phase. However, pili are essential for forming and maintaining the well-defined three-dimensional mushroom-shaped biofilm. The involvement of pili in mushroom architecture is a novel function for type IV pili in *C. crescentus*. These unique biofilm features demonstrate a spatial diversification of the *C. crescentus* population into a sessile, "stem cell"-like subpopulation (monolayer biofilm), which generates progeny cells capable of exploring the aqueous, oligotrophic environment by swimming motility and a subpopulation accumulating in large mushroom structures.**

Caulobacter crescentus is an aquatic α-proteobacterium that divides asymmetrically by giving rise to a stalked sessile cell and a motile swarmer cell (16). The replication-competent stalked cell has a different gene expression profile than the swarmer cell and bears a unique adhesive organelle, the holdfast, which allows a cell to attach to environmental surfaces. Swarmer cells uniquely express the polar flagellum and type IV pili (16). To replicate, a swarmer cell has to undergo physiological changes and develop into a stalked cell by shedding its flagellum and pili and by growing a stalk with the holdfast at its tip. Therefore, a population of *C. crescentus* cells consists of at least two physiologically distinct subpopulations: stalked cells, which are competent for a sessile biofilm life style, and swarmer cells, capable of exploring an oligotrophic environment through swimming motility. By switching between a sessile and a motile lifestyle, a population of *C. crescentus* cells enhances its chances to encounter better nutritional conditions that will allow that subpopulation to thrive and grow.

For *C. crescentus* cells, it was recently shown that the most important surface structure for adhesion to various surfaces, including glass, is the holdfast (6, 8, 31). Furthermore, by a static attachment assay, adhesion was found to be cell cycle dependent (6). Using confocal laser-scanning microscopy (CLSM) in conjunction with *gfp*-labeled cells, we show here that in a hydrodynamic flow system resembling natural freshwater streams and subsurface environments, *C. crescentus* cells form two fundamentally different types of biofilms: a monolayer biofilm and a biofilm containing densely packed, mushroom-shaped structures. Under these biofilm conditions, the holdfast structure was found to be the single most important component for attachment. Furthermore, the type IV pili were found to be critical for constructing and/or maintaining the mushroom-shaped biofilm structures.

* Corresponding author. Mailing address: James Clark Center, E 250A, 318 Campus Dr., Stanford University, Stanford, CA 94305-5429. Phone: (650) 723-3668. Fax: (650) 724-4927. E-mail: spormann@stanford.edu.

MATERIALS AND METHODS

Bacterial strains and growth conditions. Microbial materials used in this work are listed in Table 1. *Escherichia coli* strains DH5α and S17-1 were grown in Luria-Bertani medium at 37°C supplemented with ampicillin (50 μg/ml), kanamycin (25 μg/ml), gentamicin (10 μg/ml), chloramphenicol (6 μg/ml), or tetracycline (10 μg/ml), when required. Wild-type *C. crescentus* CB15 and its derivative strains were grown at 30°C in complex PYE medium (0.2% peptone, 0.1% yeast extract) or minimal M2 medium supplemented with 0.2% glucose (M2G) with 20 or 2 mM xylose (M2X) for batch or hydrodynamic biofilm experiments, respectively (10). Antibiotics were added to *Caulobacter* media at the appropriate concentration: ampicillin (10 μg/ml), kanamycin (5 μg/ml), tetracycline (1 μg/ml), and apramycin (8 μg/ml).

Strain constructions and cloning. Recombinant DNA techniques were performed according to Sambrook et al. (27). Plasmids were mobilized from *E. coli* S17-1 to *C. crescentus* by bacterial conjugation (10). To introduce Tn*7*-based *gfp* or *dsred* constructs, triparental mating was performed, and fluorescent *C. crescentus* colonies were obtained. Generalized transduction with bacteriophage φCr30 was performed as previously described (38). Phage lysates were prepared as previously described (10) from CB15 strains carrying *flgH*::Tn*5* (AS100), *flgE*::Tn*5* (AS99), pBK-mini-Tn*7*Km-*gfp*3 (AS110), miniTn*7*Km-*dsred* (AS109), and Δ*pilA-cpaF*::Ω*aac3* (AS107) mutations. UV-treated lysates were transferred into green fluorescent protein (GFP)-expressing *C. cresentus* CB15 strains or mutants via transduction.

Sau3A genomic library with genomic DNA from strain LS1088 was constructed as follows. Genomic DNA was isolated with the Bio-Rad AquaPure Genomic DNA isolation kit and was digested with Sau3A (New England Bio-

TABLE 1. Biological materials used in this work[a]

Strain or plasmid	Relevant characteristic(s)	Strain construction or reference
Strains		
E. coli		
DH5α	*recA1* Δ*lacZ*	Invitrogen
S17-1	Sm^r Tp^r *mod*$^+$ *res thi pro recA hsdR17*, integrated plasmid RP4-TC::Mu-Km::Tn*7* into genome	28
AKN67	pBK-mini-Tn*7gfp3* Km^r	19
AKN132	pBK-mini-Tn*7dsred* Gm^r Cm^r	33
AKN133	Mini-Tn*7*Km-*dsred* Km^r Sm^r Cm^r	33
C. crescentus		
CB15	Wild type; Amp^r	24
NA1000	*syn-1000*, CB15 synchronizable derivative, unable to form holdfast and rosettes	11
LS801	*flgF*::Tn*5* Km^r in CB15	L. Shapiro, unpublished data
LS1088	CC0095::Tn*5*, Km^r in CB15, holdfast deleted	L. Shapiro, unpublished data
PV14	Δ*pilA-cpaF*::Ω*aac3*, Apr^r in NA1000	35
PV35	Δ*pleA*::Δ*aac3*, Apr^r in NA1000	34
PV1735	Δ*podJ* in CB15	35
SC268	*motA102* point mutation in CB15	38
SC286	*motB108* point mutation in CB15	38
SC1035	*pleC*::Tn*5* Km^r in CB15	36
SC1119	*podJ*::Tn*5* Km^r in CB15	36
YB2878	*hfsA125* Km^r in CB15	31
AS100	*flgH*::Tn*5* Km^r in CB15	This work
AS109	miniTn*7*Km-*dsred*, Km^r in CB15	This work
AS110	pBK-mini-Tn*7gfp3* Km^r in CB15	This work
AS111	Δ*pilA-cpaF*::Ω*aac3 gfp3* Km^r Apr^r	ϕCr30 (PV14) × AS110, selected on Apr
AS112	Δ*pilA-cpaF*::Ω*aac3 motA gfp3* Km^r, Apr^r	ϕCr30 (PV14) × AS115, selected on Apr
AS113	pBK-mini-Tn*7dsred* Km^r Gm^r in YB2878	This work
AS114	pBK-mini-Tn*7dsred* Km^r Gm^r in AS100	This work
AS115	pBK-mini-Tn*7gfp3* Km^r in SC268	This work
AS116	*flgH*::Tn*5* Δ*pilA-cpaF*::Ω*aac3 gfp3* Km^r Apr^r Test^r	ϕCr30 (AS100) × AS111, selected on Tet
AS117	Δ*pilA-cpaF*::Ω*aac3 hfsA dsred* Km^r Gm^r Apr^r	ϕCr30 (PV14) × AS113, selected on Apr
AS118	*flgH*::Tn*5 hfsA dsred* Km^r Gm^r Tet^r	ϕCr30 (AS100) × AS113, selected on Tet
AS119	*motA flgH*::Tn*5* Km^r	ϕCr30 (AS100) × SC268, selected on Km
AS120	In-frame deletion of CC0095 in CB15	This work
AS121	pBK-mini-Tn*7gfp3* Km^r in AS120	This work
Plasmids		
pBluescript KS	Ap^r *lacPOZ*	Stratagene
pNPTS138	pLitmus38-derived vector with *oriT*, *sacB*, and *nptI* genes, integrates into *Caulobacter* genome, Km^r	M. R. K. Alley, unpublished data
pNPT228	pLitmus28-derived vector with *oriT* and *nptII* genes, Km^r	M. R. K. Alley, unpublished data
pHP45Ωaac3	Source of omega Apr^r cassette	5
pCRtopo4	Topoisomerase I bound covalently to the 3′-T overhangs, Km^r Amp^r	Invitrogene
pBK-mini-Tn*7gfp*3	Delivery plasmid for miniTn*7-gfp3*; *mob*$^+$ Km^r Cm^r Sm^r	19
pBK-miniTn*7dsred*	Delivery plasmid for miniTn*7-dsred*; *mob*$^+$ Gm^r Cm^r	33
miniTn*7*Km-*dsred*	Delivery plasmid for miniTn*T-dsred*; *mob*$^+$ Km^r Sm^r Cm^r	33
pRK600	Cm^r *ori*-ColE1 RK2-*mob*$^+$ RK2-*tra*$^+$ helper plasmid	17
pUX-BF13	Amp^r *mob*$^+$ *ori*-R6K; helper plasmid	3
pPE305	pCRtopo4::3′ end of CC0094 into 5′ end of CC0095	This work
pPE306	pCRtopo4::3′ end of CC0095 into 5′ end of CC0096	This work
pPE307	pNTPS138 with EcoRI-KpnI fragment containing deletion in CC0095	This work

[a] Amp,^{r}, ampicillin resistance; Km^r, kanamycin resistance; Gm^r, gentamycin resistance; Tet^r, tetracycline resistance; Apr^r, apramycin resistance; Cm^r, chloramphenicol resistance; Sm^r, streptomycin resistance.

Labs), diluted 1/200. After a 20-min incubation at 37°C, the reaction was stopped by the addition of chloroform. DNA was extracted and separated on a 0.8% agarose gel. Fragments of sizes between 4 and 8 kb were extracted with the QIAEX II gel extraction kit (QIAGEN, Alameda, Calif.). Ligation into vector pBluescript KS was performed, and clones were screened on Luria-Bertani plates containing kanamycin (25 μg/ml) and ampicillin (50 μg/ml). Clones were sequenced (PAN Facilities, Stanford University), and the sequence was compared to the National Center for Biotechnology Information database with BLASTN.

An in-frame deletion of gene CC0095 was constructed as follows. Primers CC0094, which contained an EcoRI restriction site, and CC0095Rev, with a HindIII restriction site, were used to amplify a 570-bp region including the 5′ end of gene CC0094 and 3′ end of gene CC0095. Primers CC0095Fwd with restriction site HindIII and CC0096 with restriction site KpnI were used to amplify a 420-bp fragment including the 5′ end of gene CC0095 and the 3′ end of gene CC0096, resulting in plasmids pPE305 and pPE306, respectively. Both fragments were then ligated together into the HindIII site and were cloned into vector pNPTS138, resulting in pPE307 (pNPTS138::ΔCC0095). This vector was mobilized into *C. crescentus* CB15, and first recombinants were screened on PYE kanamycin plates (10). Second recombinants were screened on PYE sucrose medium (3% end concentration), and clones were checked by PCR to confirm the successful deletion. This resulted in strain AS120.

Growth of *C. crescentus* biofilms in flow chamber. Biofilms of the *C. crescentus* wild type and its derivatives were grown on microscope coverslips attached to flow chambers with two individual channels (28 by 5 by 1 mm) at 30°C. The flow rate was maintained at 200 μl/min with a Watson-Marlow Bredel 205S peristaltic pump (Wilmington, Mass.) (18). The system was assembled prior to autoclaving. Mineral medium supplemented with 2 mM xylose was used, and the appropriate antibiotics were added. The sterile system was equilibrated with medium over-

night at a low flow rate before seeding. Precultures were prepared by inoculating a single colony from a selective plate into PYE medium supplemented with antibiotics and by incubating for 30 h at 30°C. One milliliter of cells was centrifuged, and cells were resuspended in 1 ml of 1× M2 (10). The cell density was adjusted to an optical density at 600 nm (OD_{600}) of 0.1, and 0.5 ml of this diluted cell suspension was used to inoculate a single flow channel (18). The flow was stopped for 30 min to prevent immediate washing out of the cells. Constant flow was maintained at 200 μl/min.

Biofilm imaging and image analyses. CLSM images were recorded at 24-h intervals or as indicated, until the fourth day from the middle of each channel. For each time point, 6 to 10 locations in the biofilm were chosen randomly and recorded with a Zeiss 510 laser-scanning microscope (LSM) (Carl Zeiss MicroImaging). The resolution in the *z* direction was 1.0 to 3.0 μm to minimize signal loss by sample bleaching. Scanning for all enhanced green fluorescent protein-expressing strains was conducted with the 488-nm argon laser line and with a 458- to 543-nm He/Ne laser for all DsRed fluorescence-expressing strains. Emission was measured with a band pass 500-550 filter for all enhanced green fluorescent protein-expressing strains, and a band pass 565-615 filter was used for all DsRed-expressing strains, as well as for cells labeled with wheat germ agglutinin-conjugated tetramethylrhodamine isothiocyanate (TRITC-WGA). Image analyses were performed with the IMARIS software package (Bitplane AG, Zurich, Switzerland). Quantitative analyses of the images were processed by COMSTAT software (13, 14). The mean value was calculated from 6 to 10 independently taken images per time point.

Staining of biofilms in flow chambers. The holdfast was stained with TRITC-WGA (Sigma) as previously described (31) with modifications. The labeled lectin specifically binds to the holdfast and was visualized by CLSM. Twenty microliters of a stock solution of TRITC-WGA (0.5 mg/ml) was injected into the flow cell after the flow was stopped. After a 15-min incubation at room temperature in the dark, the flow was restored and the residual dye was washed out.

Bacterial viability was determined by using LIVE/DEAD *Bac*Light bacterial viability kit (Molecular Probes, Inc., Eugene, Oreg.). Three microliters of component A and 3 μl of component B were mixed and injected into one channel with biofilm while the flow was stopped. Samples were incubated for 15 min at room temperature in the dark and then the flow was restored to wash out the unbound dye.

Twitching test. Twitching assays were performed according to a previously published protocol (2), with modifications. Plates with different agar concentrations (0.5, 0.6, 0.8, and 0.9%) were used to examine twitching motility but not swarming. Cells from a single colony inoculum were stabbed to the bottom of M2G agar plates (0.5, 0.6, 0.8, and 0.9%) and incubated for 2 days at 30°C and for 4 additional days at room temperature to reduce active growth but to favor twitching motility in the interstitial zone at the agar-petri dish interface. The twitching zone was stained with Coomassie blue R250 and distained (27).

RESULTS

***C. crescentus* CB15 wild-type biofilms.** *C. crescentus* biofilms were studied in a hydrodynamic flow chamber system with a mineral medium containing 2 mM xylose as an electron and carbon source. Flow chambers were seeded with exponentially growing *gfp*- or *dsred*-tagged cells that were diluted to OD_{600} of about 0.1 in fresh mineral medium prior to injection. After 30 min of incubation under static conditions, flow was initiated to a rate of 200 μl/min, and biofilms were visualized by CLSM at 24-h intervals for up to 120 h. Figure 1 shows representative time course images of developing *C. cresentus* CB15 (AS110) biofilms. The confocal image stacks were quantified using COMSTAT (14), and the biofilm parameters determined are summarized in Fig. 2. During the first 24 h, single cells were visible on the glass surface predominantly as isolated cells. After 48 h, the surface coverage increased. The density of those monolayers did not increase significantly until after 72 h. Even after 96 h, uncovered areas were present, suggesting that lateral spreading of *C. crescentus* cells on the glass surface is minimal. In the later stages (>5 days), however, a noticeable increase in the monolayer density was observed.

In addition to, and probably independent of, the monolayer biofilm, a dynamic development of isolated microcolonies and mushroom-shaped structures was noticed (Fig. 1, 96 and 120 h). Microcolonies, which at 48 h contained a few hundred cells, gave rise to mushroom-shaped structures at 72 h. The areas between those structures were either uncovered, covered by cell monolayers, or covered by isolated microcolonies containing only a few cells. At 72 and 96 h, most biomass accumulation had occurred in the microcolonies and mushroom-shaped structures. The latter structures (>6 days) were frequently observed to reach a thickness of up to several hundred micrometers (data not shown). This continuous increase in biomass in the microcolonies and mushrooms is reflected in the quantitative biofilm data in Fig. 2. As evident in this figure, a significant increase in biomass was observed between days 3 and 4. It therefore appears that *C. crescentus* forms a biphasic biofilm under hydrodynamic conditions: a flat-cell monolayer biofilm intermixed with a biofilm consisting of extensive three-dimensional mushroom-shaped structure. This heterogeneity of the overall biofilm is reflected in the large standard deviation of the biomass and average thickness parameter, respectively (Fig. 2). Only in later stages (after day 7) did cell monolayers cover the entire area between mushrooms, and continued incubation of the flow chamber system until day 8 (data not shown) resulted in detachment of the large mushroom-shaped structures, presumably due to shear stress and/or loss of viability of the mushroom structures (see below).

The absence of a significant overall increase in biofilm mass and thickness until day 4 and the apparent dual nature of *C. crescentus* biofilms, both as a flat monolayer or as localized growth of pronounced mushrooms, is unique compared to the well-characterized biofilms of γ-proteobacteria. Specifically, the apparent absence of net growth (i.e., biomass accumulation) of the monolayer biofilm raises several obvious questions, including (i) whether the monolayer consists mainly of non-growing swarmer cells that are unable to differentiate into stalk cells, (ii) whether the monolayer consists predominantly of stalked cells that do not grow or grow only at a very slow rate, or (iii) whether the monolayer consists predominantly of stalked cells that are active and grow but with the emerging swarmer cells not retained in the biofilm monolayer. To distinguish between these possibilities, we investigated the cells in the monolayer for viability and for the presence of the stalk cell-specific holdfast structure.

The *C. crescentus* holdfast is composed of polysaccharides including *N*-acetylglucosamine (8). WGA binds specifically and stably to the *N*-acetylglucosamine component of this polysaccharide (31). We used TRITC-conjugated WGA to fluorescently stain the holdfast and to identify thereby holdfast-carrying stalked cells in the monolayer biofilm. Monolayer cells of strain CB15 were found to predominantly carry a holdfast and to attach to the glass surface (Fig. 3A and B). However, some surface-associated cells (about 30%) did not stain with TRITC-WGA (Fig. 3C).

To examine whether the cell monolayer consists of active or inactive cells, we used the LIVE/DEAD staining kit, consisting of two nucleic acid binding dyes, the membrane permeable green-fluorescent dye SYTO-9, and the membrane-impermeable dye propidium iodide (Molecular Probes, Inc.). Cells with intact membranes will exhibit a green fluorescence due to SYTO-9 staining, whereas cells that emit red fluorescence will

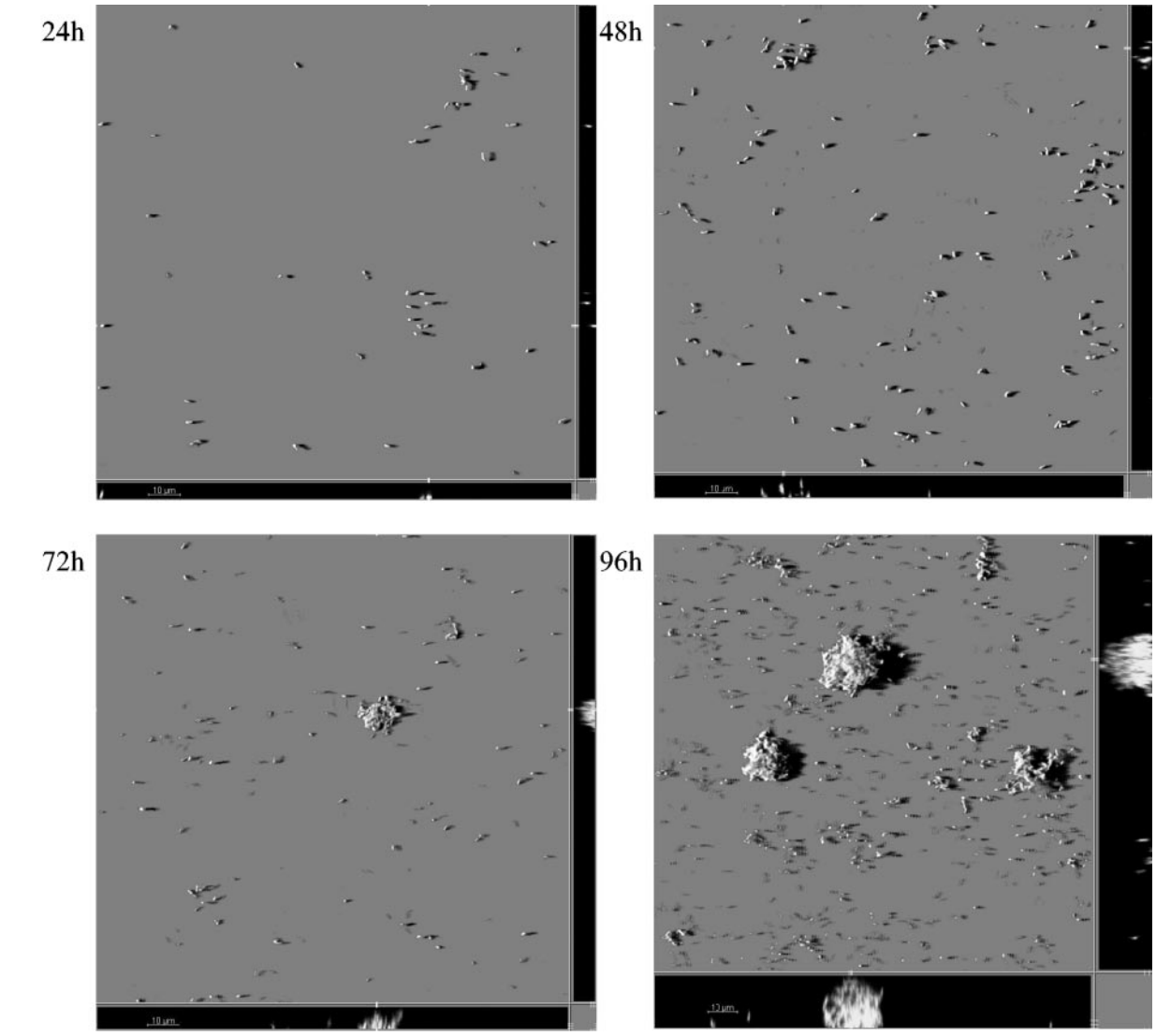

FIG. 1. Time course of *C. crescentus* CB15 (AS110) biofilm formation. Cells were grown in flow chambers under a constant flow of 200 μl/min in minimal medium supplemented with 2 mM xylose as a single carbon source at 30°C. Images were taken by CLSM. Images display shadow projections of AS110 biofilms; *x-z* and *y-z* sagittal images at selected positions in the biofilm are shown at the bottom and right sides of images, respectively.

do so because of the predominance of propidium iodide and are inferred to be devoid of an intact cytoplasmic membrane (i.e., inactive or "dead"). *C. crescentus* CB15 biofilms were grown for 48 h in the hydrodynamic flow chamber and stained with the LIVE/DEAD stain (Fig. 4). About 70% of all cells in the biofilm monolayer stained as "live" and were consequently considered to be active and replication competent; 25 to 30% of all cells stained dead. Microcolonies were found to comprised predominantly viable cells (Fig. 4A). For comparison, we investigated cells growing to mid-log phase (OD_{600} = 0.28) in batch cultures in 20 mM M2X medium and found that about 7% of the cells stained as dead. It seems therefore unlikely that all dead cells in the biofilm chamber originated solely from the inoculum. Instead, they presumably resulted from senescence

of surface-attached cells (1). We also observed that 96-h-old mushroom-shaped structures (10 to 20 μm in thickness) consisted predominantly of green fluorescent cells (Fig. 4B). However, larger mushrooms (≥100 μm) contained a core of cells that stained as dead while cells at the periphery stained as live (Fig. 4C). These observations showed that the monolayer biofilm as well as the mushroom-shaped biofilm consist of active, stalked cells. In addition, these data also support the notion that the detachment of larger mushroom structures in later biofilm stages (after day 6) might be due to a weakening of the mushroom structure due to cell death.

To test whether the pronounced mushroom structures originated by clonal growth of an attached cell (18) or by aggregation of individual cells on the surface, as suggested for *P. aeruginosa* (23), we performed biofilm experiments with mixtures of *gfp*- and *dsred*-labeled cells. The two isogenic strains, AS110 and AS109, were mixed in equal ratios before a diluted suspension was injected to seed the flow chamber. After 96 h of growth, the biofilm was inspected by CLSM, and representative images are shown in Fig. 5. Microcolonies emitted either red or green fluorescence, and no hybrid microcolonies were found. These observations demonstrate that microcolony formation and, most likely, subsequent mushroom formation of *C. crescentus* CB15 resulted from clonal growth of individual cells or cell clusters and that no migration and mixing of cell populations on the surface preceded mushroom formation. At later time points (>5 days; data not shown) single green fluorescent cells could be found at the outside of red fluorescing mushrooms and vice versa, which could have resulted from attachment of swarmer cells that were released from upstream sections of the flow chamber. From the observation above, we concluded that the mushroom-shaped structures in *C. crescentus* biofilms resulted from clonal growth.

Biofilm formation of *C. crescentus* CB15 mutants. Flagellum-dependent motility as well as pili have been shown to play roles at several stages in biofilm formation in *P. aeruginosa*, *E. coli*, *Vibrio cholerae*, and *Shewanella oneidensis* (18, 23, 26, 32, 37). Because the polar flagellum and type IV pili in *C. crescentus* are formed only in the swarmer cell type, we investigated the effect of mutations in these extracellular structures on initial attachment and biofilm development. We also investigated the function of the unique holdfast structure in *C. crescentus* biofilm formation.

Holdfast is important for the initial attachment. Because *C. crescentus* cells carry the holdfast at the tip of the stalk, we investigated the role of the holdfast in biofilm formation of *C. crescentus* developing in a hydrodynamic flow chamber system. We tested a *hfsA* mutant (AS113) that carries a defect in holdfast biosynthesis (31). As evident in Fig. 6 and 7A, the *hfsA* (AS113) transposon mutant cells were defective in attachment and biofilm formation (tested until 96 h). The few adhering cells formed loosely associated microcolonies, which did not progress into mushroom-shaped structures.

Transposon mutant strain LS1088, originally identified as holdfast deficient in the laboratory of Lucy Shapiro (unpublished data), was found to be defective in rosette formation and unable to bind lectin (L. Shapiro, personal communication). Microtiter plate assays showed that biofilm formation was reduced to less than 10% of the wild type (data not shown). A Sau3A genomic library was constructed, and the site of transposon insertion was determined by sequencing. The Tn*5* insertion was found to be in open reading frame (ORF) CC0095. This ORF was annotated as expressing a WecB/TagA/CpsF family protein. In *E. coli* (4), *Salmonella enterica* (9), and

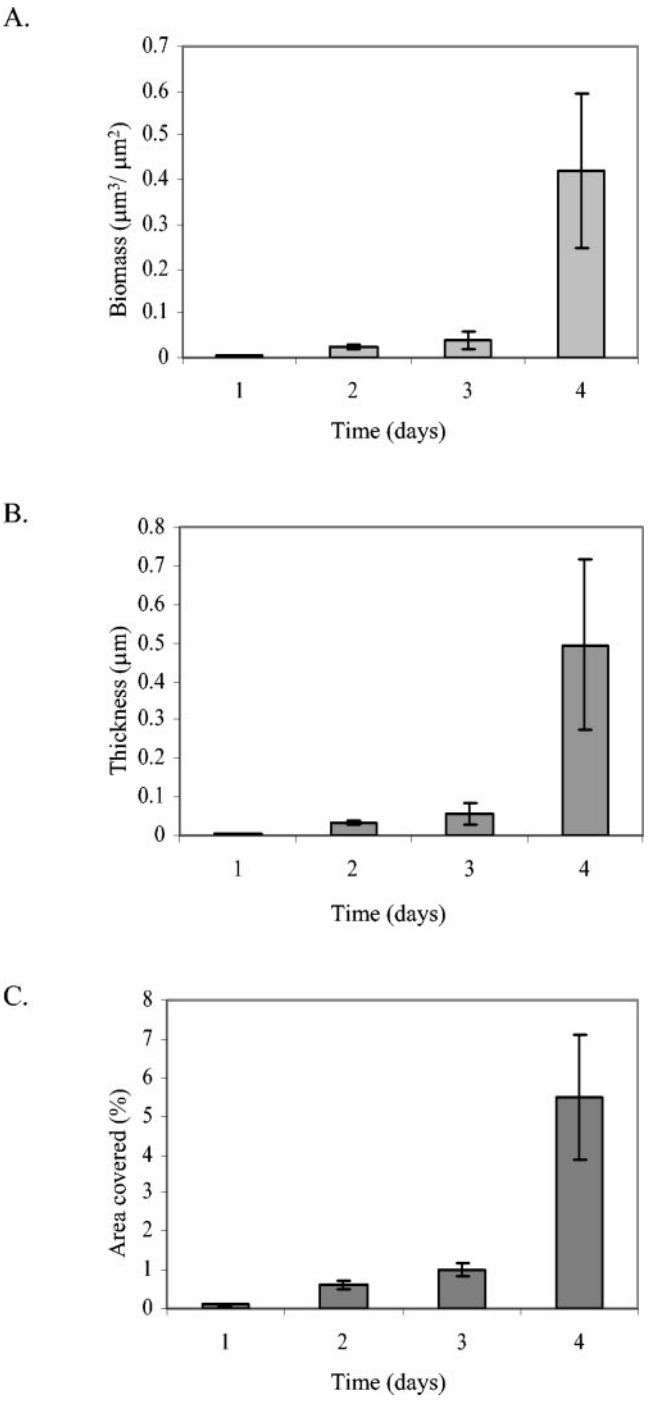

FIG. 2. Quantification of *C. crescentus* CB15 (AS110) biofilm development by COMSTAT. Data have been taken from Fig. 1. (A) Total biomass (cubic micrometers per square micrometers) accumulating on an area of 146 μm^2; (B) thickness in micrometers of the biofilm is an average thickness, including monolayers and mushroom-shaped structures in a area of 146 μm^2; (C) percent area covered by all cells that are attached to the glass surface in an area of 146 μm^2.

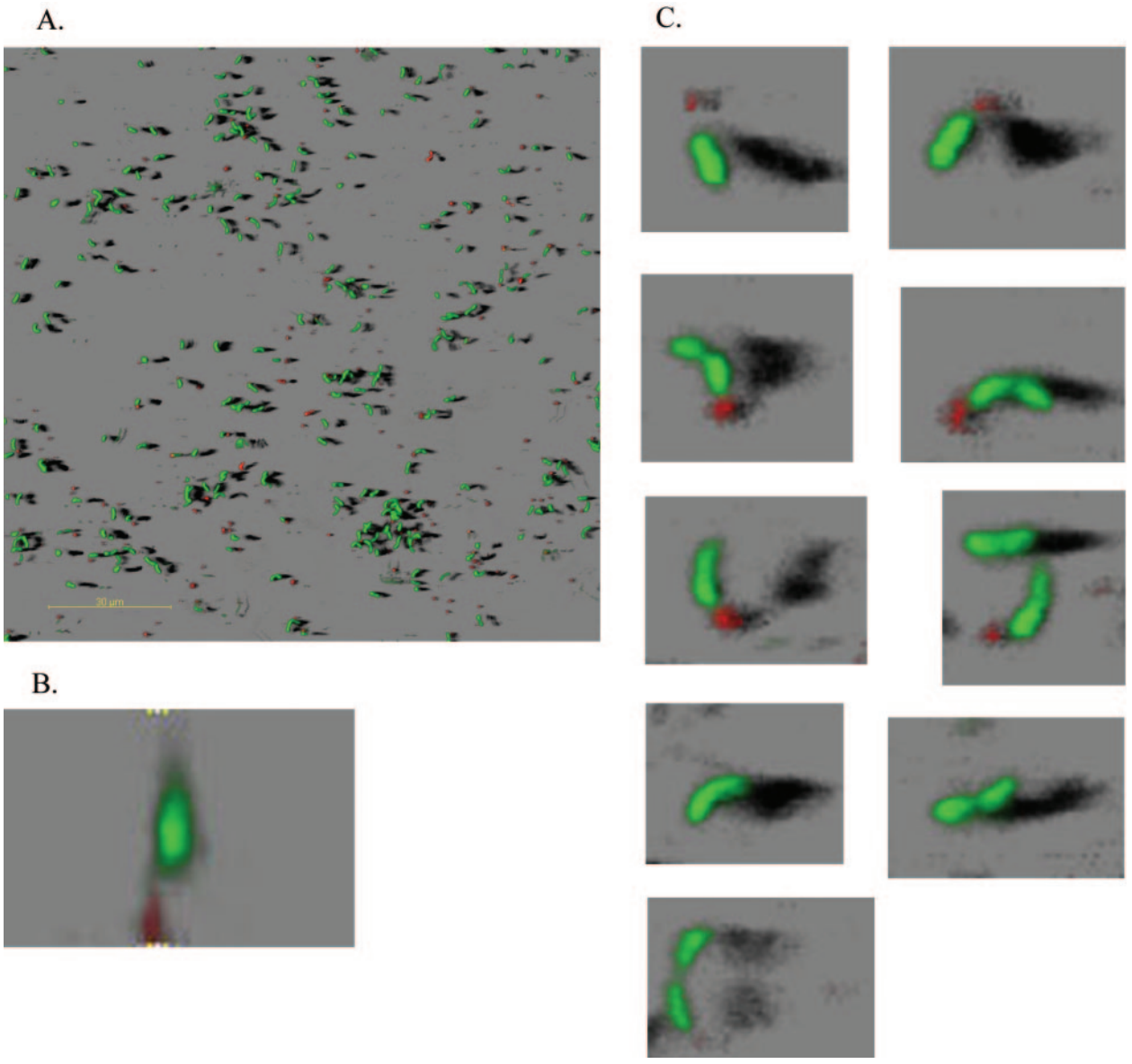

FIG. 3. Visualization of holdfast on surface-associated *C. crescentus* CB15 cells. Biofilms were stained with TRITC-WGA, and images were recorded at the substrate-biofilm interface. (A) Shadow projection. Bar, 30 μm. (B) Lateral view of a cross-section through a stalked cell that is attached to the surface. (C) Single cells attached on the surface.

Pseudomonas aeruginosa (7), the *wecB* gene encodes UDP-*N*-acetylglucosamine-2-epimerase, and thus it is involved in the conversion of UDP-*N*-acetyl-glucosamine to UDP-*N*-acetyl-mannosamine. This is a central step in the biosynthesis of enterobacterial common antigen. In *C. crescentus*, however, the function of the WecB-like protein is not yet understood (unpublished data). The Tn*5* insertion was transduced into *C. crescentus* CB15, and the same phenotype was observed as for LS1088. An in-frame deletion of ORF CC0095 was introduced in strain CB15, resulting in strain AS120, which was found to be negative for rosette formation, binding to TRITC-WGA, and biofilm formation in microtiter plates (data not shown). Biofilm formation in the *gfp* gene-labeled derivative of AS120, strain AS121, was studied under hydrodynamic conditions, and a phenotype similar to the *hfsA* (AS113) mutant was observed (Fig. 6 and 7A). From these results, we conclude that the holdfast plays an essential role in the initial adhesion process in *C. crescentus* CB15.

Swarmer cells are able to attach to surfaces by means of their flagellum. A flagellum mutant defective in the *flgH* gene (AS114) was constructed and tested in the hydrodynamic biofilm system. As evident in Fig. 6 and 7A, the mutant is defective in the initial attachment, suggesting that the flagellum is important for initiating and/or maintaining successful contact to the inorganic surface. However, monolayer biofilms did develop until day 4, including microcolonies. Interestingly, the surface coverage of the *flgH* mutant (AS114) was more pronounced than that of the wild type (Fig. 6). This statement is not supported numerically by the COMSTAT analyses, due to the fact that the biomass of the wild type is averaged over the

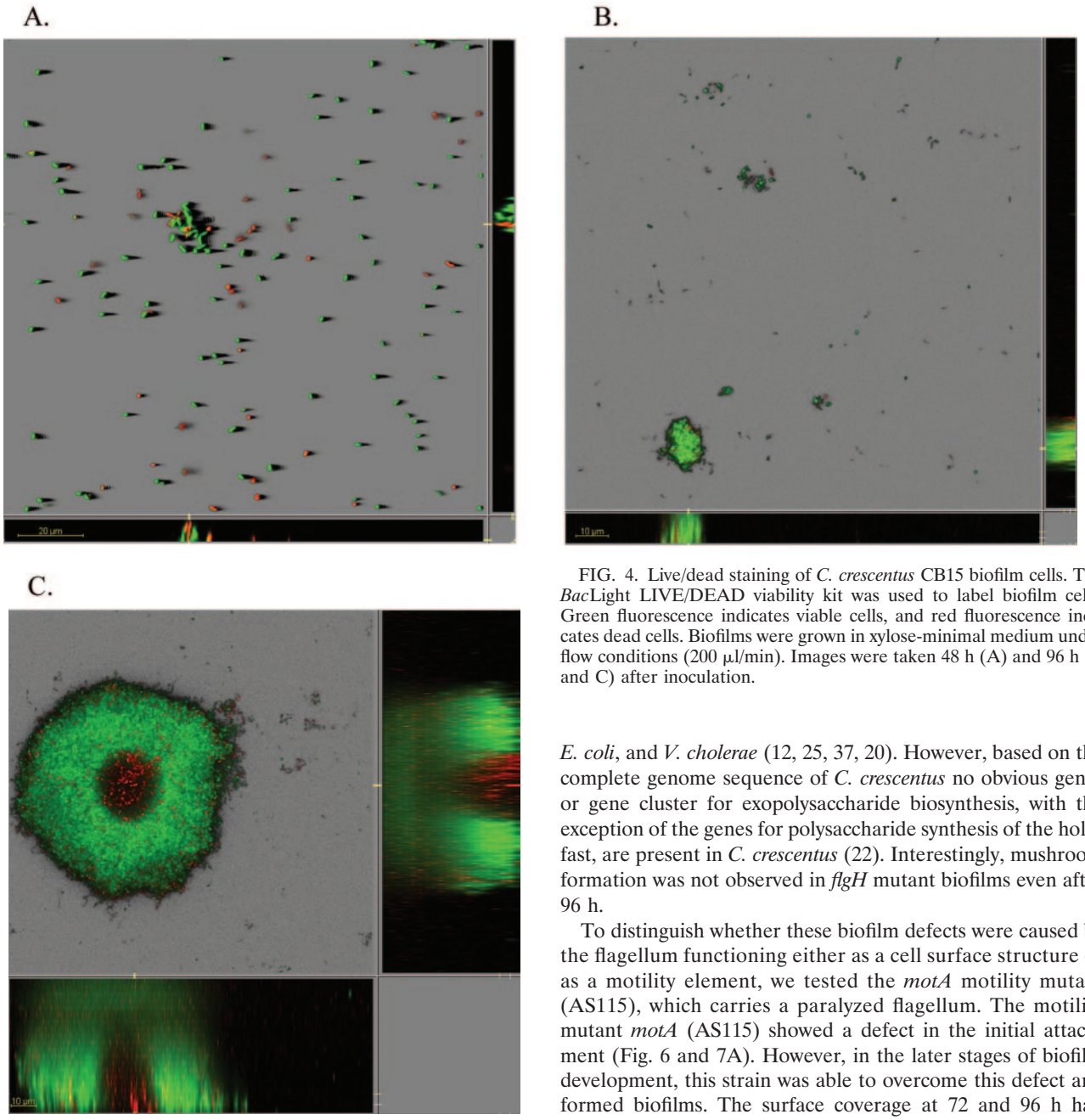

FIG. 4. Live/dead staining of *C. crescentus* CB15 biofilm cells. The *Bac*Light LIVE/DEAD viability kit was used to label biofilm cells. Green fluorescence indicates viable cells, and red fluorescence indicates dead cells. Biofilms were grown in xylose-minimal medium under flow conditions (200 μl/min). Images were taken 48 h (A) and 96 h (B and C) after inoculation.

area covered by cell monolayers and mushroom-shaped structures, which gives rise to the large standard deviation. In the *flgH* mutant, mushroom-shaped structures do not form. However, we could observe that the *flgH* cell monolayers were denser than the monolayers in the wild type (Fig. 6). This fact could indicate that the flagellum might play a role in the escape of cells from the biofilm in the later stages. In the absence of the flagellum, progeny swarmer cells could be impaired in leaving the biofilm and consequently form thicker, more homogeneous monolayers. An alternative explanation for the enhanced monolayer biofilm could be an inversely correlated regulation of flagella biosynthesis and exopolysaccharide production similar as to what has been observed in *P. aeruginosa*, *E. coli*, and *V. cholerae* (12, 25, 37, 20). However, based on the complete genome sequence of *C. crescentus* no obvious genes or gene cluster for exopolysaccharide biosynthesis, with the exception of the genes for polysaccharide synthesis of the holdfast, are present in *C. crescentus* (22). Interestingly, mushroom formation was not observed in *flgH* mutant biofilms even after 96 h.

To distinguish whether these biofilm defects were caused by the flagellum functioning either as a cell surface structure or as a motility element, we tested the *motA* motility mutant (AS115), which carries a paralyzed flagellum. The motility mutant *motA* (AS115) showed a defect in the initial attachment (Fig. 6 and 7A). However, in the later stages of biofilm development, this strain was able to overcome this defect and formed biofilms. The surface coverage at 72 and 96 h had increased and was comparable to that of the wild type (data not shown). The *motA* mutant (AS115) formed microcolonies and mushroom-shaped structures, although they never reach the thickness of the wild type (Fig. 8). The fact that *motA* is able to form some mushroom-shaped structures indicates a role of the flagellum as a cell appendage in the three-dimensional biofilm structure. In summary, the observations show that the flagellum and flagellum-dependent motility not only support the initial adhesion event but also are involved in the transition from microcolonies to mushroom-shaped structures and thus in forming and/or maintaining the three-dimensional structure.

Pili are involved in the maintaining the biofilm structure. Type IV pili are present only on *C. crescentus* swarmer cells, and their only known functions to date are to mediate infection by phages ϕCb5 and ϕCbK (29) and adhesion to plastic sur-

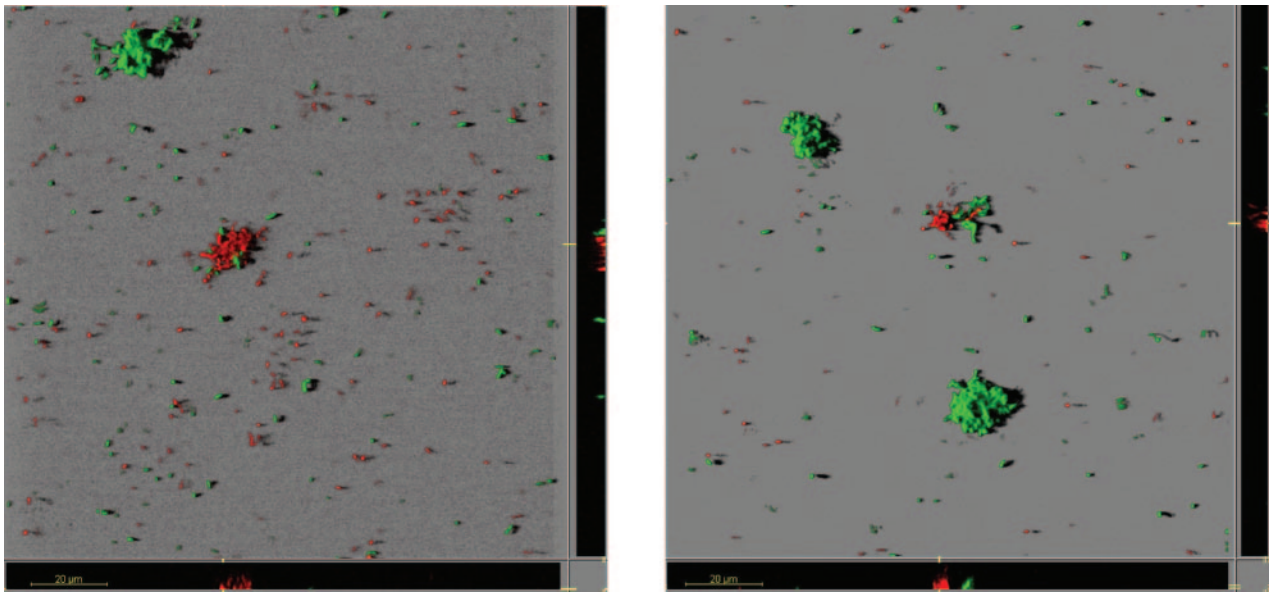

FIG. 5. Clonal growth of *C. crescentus* CB15 microcolonies. Experiments were initiated by seeding biofilm chambers with a 1:1 mixture of *gfp*- and *dsred*-tagged *C. crescentus* wild-type cells (AS110 and AS109). Biofilms were irrigated at a flow rate of 200 μl/min in xylose-minimal medium at 30°C. Images were recorded after 96 h.

faces (6). Type IV pili are known in other microbes to be involved in surface-dependent twitching motility (2, 23), and this phenotype has been associated with a putative role of these appendages in biofilm architecture (18, 23, 26, 37). We investigated whether *C. crescentus* CB15 cells are able to move by type IV pilus-dependent twitching motility, as described in Materials and Methods. Testing 0.5, 0.6, 0.8, and 0.9% agar M2G plates (2), we were unable to find conditions where twitching motility could be visualized as a spreading on the plastic surface of a petri dish. Agar concentrations of 0.8 and 0.9% were sufficient to suppress swarming motility, but after Coomassie staining no twitching zone could be determined. This observation led to the conclusion that *C. crescentus* CB15 is unable to twitch under those assay conditions.

Studies of other biofilm forming bacteria have shown that pili are important for the colonization of substrates (18, 23, 26, 37). We investigated different *C. crescentus* pilus-deficient mutants with respect to biofilm formation. A deletion mutant that lacks all genes required for pilus assembly and for the pilin subunits (AS111) was grown under hydrodynamic conditions. Representative biofilm images from a time course are presented in Fig. 6. The initial attachment phase after 24 h of AS111 was similar to that of the wild type (AS110) (Fig. 6 and 7A). This indicates that pili are not crucial for the initial attachment to surfaces. However, during subsequent development AS111 displayed noticeable differences from wild-type strain AS110. Differences in the shape of microcolony became apparent after 3 days. The pili mutant developed "mottled" structures, in which cells appeared loosely associated to each other and did not develop into dense mushroom-shaped structures during the 96-h time course. From these observations, we concluded that the *C. crescentus* type IV pili play a critical role during maturation of the mushroom-shaped biofilm and are required to support the compact mushroom-shaped structures.

The biofilm phenotype of the *hfsA flgH* double mutant (AS118) demonstrates that pili, which are the only known extracellular appendages remaining in this strain, are not sufficient for the initial attachment and supports the finding that the holdfast and flagellum are crucial for early biofilm formation. This double mutant was completely impaired in biofilm formation during the time course of 4 days (Fig. 6 and 7A).

DISCUSSION

***C. crescentus* biofilm development.** This is the first study to examine the biology of *C. crescentus* CB15 in biofilms developing in mineral medium under chemostate-like, hydrodynamic conditions, which reflects the natural environmental condition of this oligotrophic freshwater bacterium. Previous studies have examined adhesion of cells to plastic or glass surfaces in a static, rich medium (6, 30). Furthermore, the present report examined for the first time the development of *C. crescentus* biofilms using CLSM, which allowed us to conduct noninvasive, single-cell resolution observations. The analysis of mutants defective in cell appendages, such as flagella, pili, and the holdfast structure revealed the relative importance of these elements in the initial and later phases of biofilm formation.

One of the striking features observed in *C. crescentus* is the formation of biphasic biofilms: relatively stable cell monolayers and symmetrical mushroom-shaped structures with pronounced three-dimensional architecture (Fig. 1 and 9). Monolayer biofilms established within the first day and remained in this architecture for at least 5 days. The monolayers consisted

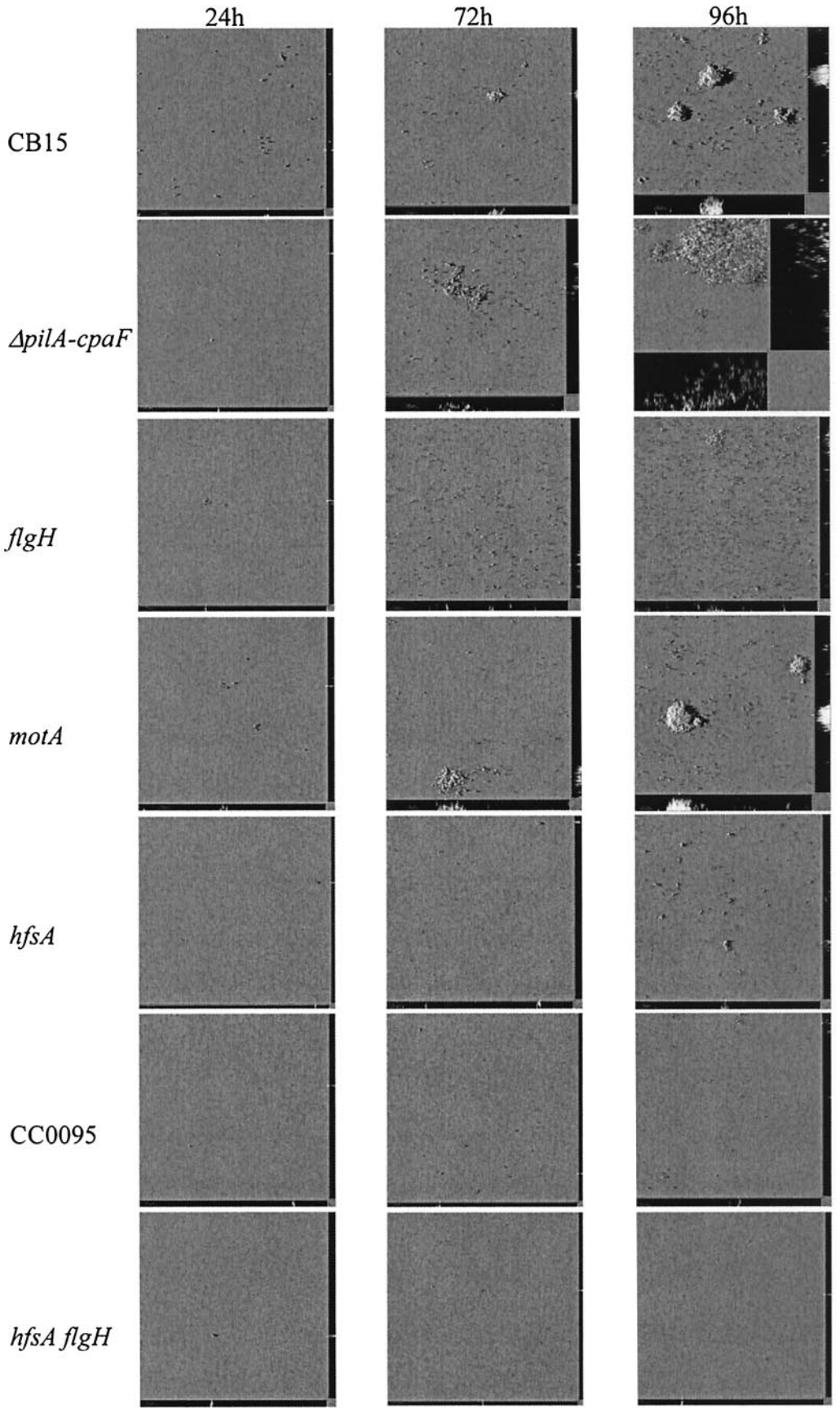

FIG. 6. Time course of biofilms of *C. crescentus* mutants defective in various extracellular appendages. Shadow projections of CLSM images are shown: single mutants in a pilus locus (AS111 [Δ*pilA-cpaF*::Ω*aac3*]), *flgH* (AS114), *motA* (AS115), *hfsA* (AS113), and CC0095 (AS121) genes and double-mutant *hfsA flgH* (AS118).

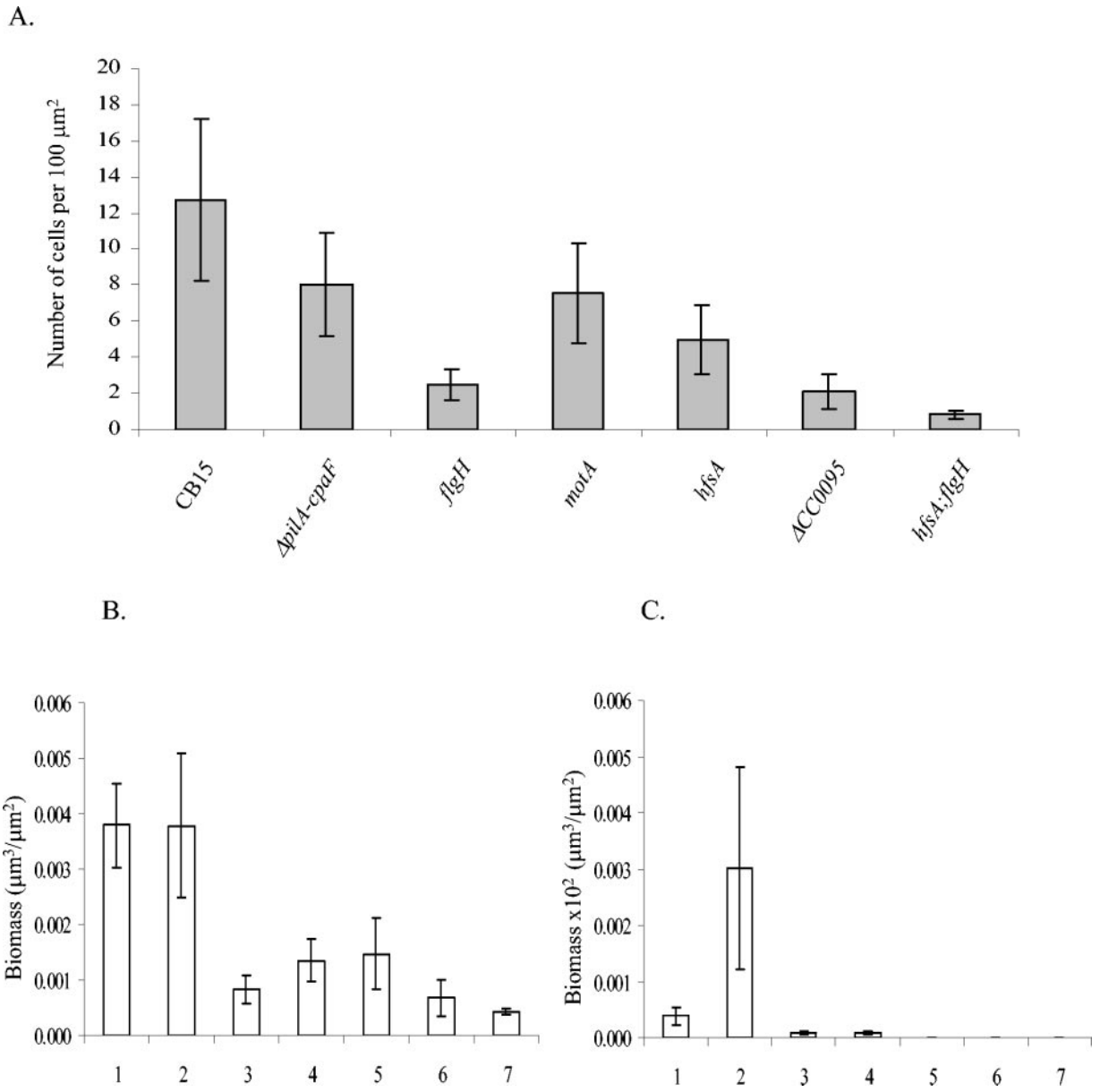

FIG. 7. Attachment of *C. crescentus* cells to a glass surface. (A) Number of cells attached to the substrate per 100 μm^2 after 24 h. (B and C) Quantitative COMSTAT analyses of biofilms: *C. crescentus* CB15 (lanes 1) is compared with Δ*pilA-cpaF*::Ω*aac3* (AS111) (lanes 2), *flgH* (AS114) (lanes 3), *motA* (AS115) (lanes 4), *hfsA* (AS113) (lanes 5), ΔCC0095 (AS121) (lanes 6), and double *hfsA flgH* (AS118) (lanes 7) mutants. Biomass (in cubic micrometers per square micrometers) was determined at 24 h (B) and 96 h (C). Note the difference in the ordinate scales in panels B and C, respectively.

mainly of stalked cells (Fig. 3) that adhered to the silicate surface by means of the holdfast. The holdfast structure is the dominant cellular adhesin mediating cell-surface contact, as revealed by analysis of *hfs* mutants (Fig. 6), and was found previously to be important also in a static system (6, 8, 31). Monolayer cells are active, as indicated by the positive live/dead staining (Fig. 4), and replication competent, as revealed by the presence of numerous predivisional cells (Fig. 3A). In addition, the finding that the cell monolayers increased in thickness in *motA* and *flgH* mutant biofilms (AS115 and AS114) suggests that these monolayer cells do grow and generate swarmer cells. Each new cell cycle of a dividing monolayer cell produces new swarmer cells, which could be retained in the biofilm, leading to an increase in thickness, or could separate from the monolayer biofilm by swimming. The biofilm phenotype of the motility mutants suggests that motility is required for swarmer cells to escape from the monolayer biofilm in the hydrodynamic system. Therefore, cells in the monolayer biofilm act as stem cells and generate swarmer cells, which depart from that biofilm and can attach at downstream surfaces, including microcolonies and mushrooms in the flow cell system. Considering a maximum average doubling time of about 24 h, as inferred from the increase in biomass of mushrooms, monolayer cells go through a minimum of four cell

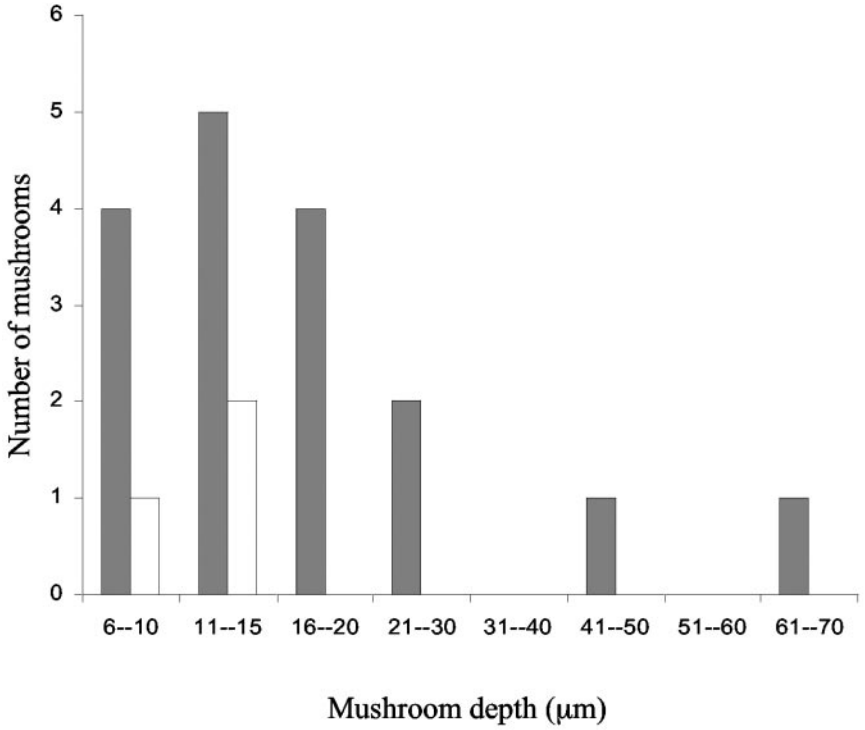

FIG. 8. Mushroom density of the *C. crescentus* wild type (AS110) and *motA* mutant (AS115). Density was determined on day 4 after growth in minimal medium with a flow rate of 200 μl/min. Numbers of wild-type mushrooms are presented in dark gray bars and of the *motA* mutant in white bars. At least three representative CLSM images were analyzed per strain, and the area measured per image was 146 μm^2.

divisions within the first 4 days. As the live/dead staining experiment indicates, senescence might be a significant parameter of the monolayer biofilm. Our biofilm system may, therefore, represent a useful system to study the life cycle of individual *C. crescentus* cells with respect to senescence.

In addition to the monolayer biofilm, microcolonies and symmetrical mushroom-shaped structures, which are clearly distinct from the monolayer, appeared on the silicate surface. These mushroom-shaped structures were derived by clonal growth of individual cells or cell clusters that attached to the surface (Fig. 5). Because of the net increase in biomass, the swarmer cells formed in the microcolonies were retained in these biofilms. Analysis of the holdfast, motility, and pilus mutants clearly indicated that these extracellular appendages are necessary for forming and/or maintaining these structures. The holdfast is also required for rosette formation, where 5 to 10 stalked cells are attached to each other at the tip of their stalks, presumably by the holdfast (15). Holdfast mutants do not form rosettes (8, 31). As our experiments were conducted with the *C. crescentus* CB15 wild type, a small fraction of the liquid-grown inoculum cells might have been present as rosettes, as revealed by microscopic observations (data not shown). It is conceivable that the subpopulation of the stalked cells existing in form of rosettes may form the origin of the microcolonies and mushroom structures observed. However, after 24 h, we did not readily observe rosettes consisting of more than five cells on the glass surface.

In addition to the holdfast structure, the polar flagellum seems to be necessary for microcolony and mushroom formation under hydrodynamic conditions (Fig. 6). For other microbial systems, flagella have been shown to be involved in various steps of biofilm formation (18, 23, 26, 32, 37). The involvement of the flagellum in microcolony and mushroom formation of *C. crescentus* biofilms suggests that the flagellum structure in the newly developing swarmer cells is required for retaining this subpopulation in the mushrooms. This function is distinct from the potential role of the flagellum in monolayer biofilms, which is to aid in cells' escaping from monolayer biofilms. Apparently, this is not the case in microcolonies and mushroom structures, and the flagellum may function as an adhesin. This dual function of the flagellum together with the profoundly different morphology suggest that the microcolonies and mushroom-shaped structures may be comprised of a physiologically, and perhaps genetically distinct subpopulation in the biofilm.

Like flagella, type IV pili have been shown to be involved in biofilm formation in various systems (18, 23, 32). In addition to mediating critical attachment, type IV pilus-dependent twitching motility was identified as a means for cells to move in a developing biofilm and to control its architecture (18). The mode of action of type IV pilus-dependent motility is by energy-dependent retraction of the pili, which thereby shortens the distance between the piliated cell and the biotic or abiotic surface to which the pili attach (21). We have found that *C. crescentus pil* mutants are not severely defective in attachment. Although these pili may contribute to the initial adhesion, the most pronounced phenotype was on the mushroom structure (Fig. 6). The mushroom structures of *pil* mutant cells had lost the high cell density and consisted of a network of loosely associated cells. These mottled mushrooms were asym-

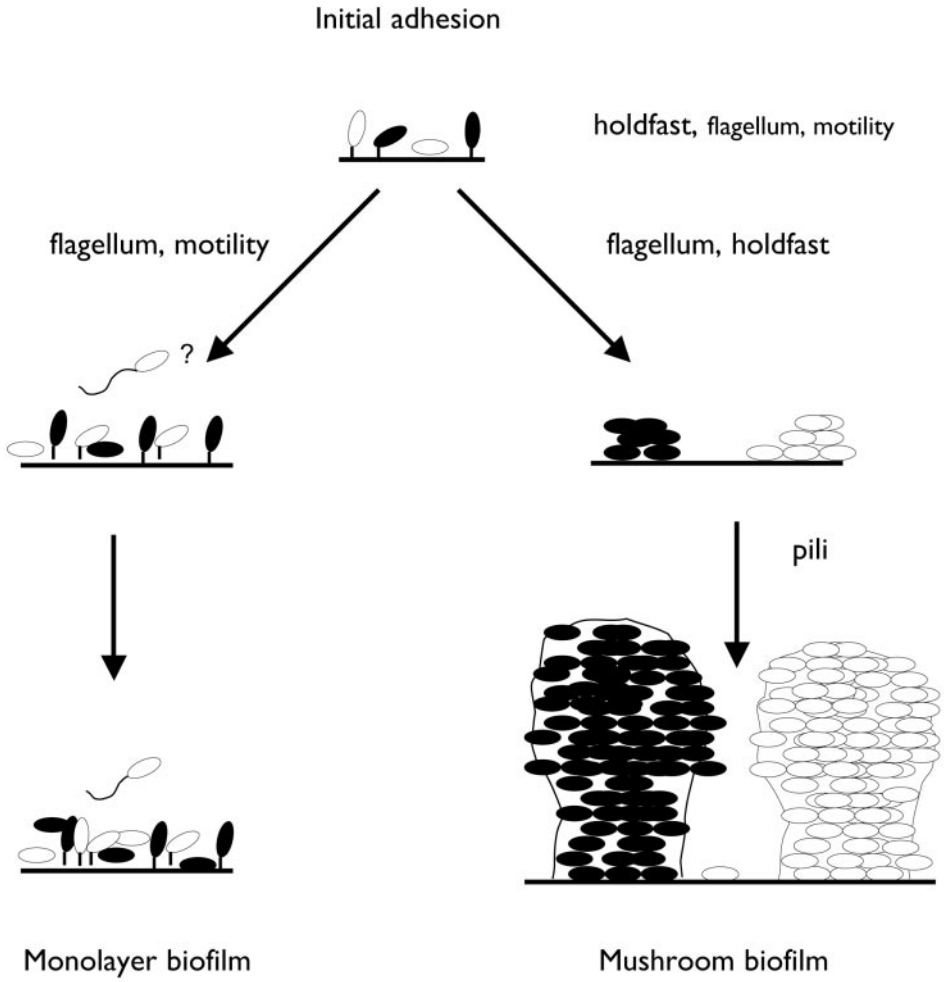

FIG. 9. Biphasic biofilms of *C. crescentus*. Two types of biofilms can be observed to develop on a glass surface in a hydrodynamic flow chamber system: a cell monolayer biofilm and a biofilm consisting of substantial three-dimensional mushroom-shaped structures. Extracellular appendages relevant for the respective stages of biofilm formation are indicated. See Discussion for detailed explanations.

metric and loosely protruded into the lumen of the flow chamber. While we were unable to show that *C. crescentus* cells are capable of moving by twitching motility on a plastic surface, these pili might be biologically active in mediating tight cell-cell contact. If, as in the *pil* mutants, this interaction is disrupted, the absence of such interaction leaves mushrooms appearing amorphous. These observations may also suggest that the maintenance of a condensed mushroom structure requires the energy-dependent activity of retracting pili.

ACKNOWLEDGMENTS

We thank Lucy Shapiro, Harley McAdams, and Yves Brun and their laboratories, as well as Patrick Vollier for providing strains and helpful discussions. We especially thank Craig Stephens for helpful discussions and for critically reading the manuscript. We are grateful to Søren Molin for providing the Tn*7*-based *gfp* and *dsred* constructs and for many discussions. We thank members of the Spormann laboratory for critical discussions and Lori Howe for technical support at the Stanford Biofilm Research Center. We also thank an anonymous reviewer for useful comments.

This work was supported by a GTL grant from DOE.

REFERENCES

1. **Ackermann, M., S. C. Stearns, and U. Jenal.** 2003. Senescence in a bacterium with asymmetric division. Science **300:**1920.
2. **Alm, R. A., and J. S. Mattick.** 1996. Identification of two genes with prepilin-like leader sequences involved in type 4 fimbrial biogenesis in *Pseudomonas aeruginosa.* J. Bacteriol. **178:**3809–3817.
3. **Bao, Y., D. P. Lies, H. Fu, and G. P. Roberts.** 1991. An improved Tn7-based system for the single-copy insertion of cloned genes into chromosomes of gram-negative bacteria. Gene **109:**167–168.
4. **Barua, S., T. Yamashino, T. Hasegawa, K. Yokoyama, K. Torii, and M. Ohta.** 2002. Involvement of surface polysaccharides in the organic acid resistance of Shiga toxin-producing Escherichia coli O157:H7. Mol. Microbiol. **43:**629–640.
5. **Blondelet-Rouault, M. H., J. Weiser, A. Lebrihi, P. Branny, and J. L. Pernodet.** 1997. Antibiotic resistance gene cassettes derived from the omega interposon for use in E. coli and Streptomyces. Gene **190:**315–317.
6. **Bodenmiller, D., E. Toh, and Y. V. Brun.** 2004. Development of surface adhesion in *Caulobacter crescentus*. J. Bacteriol. **186:**1438–1447.
7. **Burrows, L. L., K. E. Pigeon, and J. S. Lam.** 2000. *Pseudomonas aeruginosa* B-band lipopolysaccharide genes *wbpA* and *wbpI* and their Escherichia coli homologues *wecC* and *wecB* are not functionally interchangeable. FEMS Microbiol. Lett. **189:**135–141.
8. **Cole, J. L., G. G. Hardy, D. Bodenmiller, E. Toh, A. Hinz, and Y. V. Brun.** 2003. The HfaB and HfaD adhesion proteins of *Caulobacter crescentus* are localized in the stalk. Mol. Microbiol. **49:**1671–1683.
9. **Danese, P. N., G. R. Oliver, K. Barr, G. D. Bowman, P. D. Rick, and T. J. Silhavy.** 1998. Accumulation of the enterobacterial common antigen lipid II biosynthetic intermediate stimulates *degP* transcription in *Escherichia coli.* J. Bacteriol. **180:**5875–5884.
10. **Ely, B.** 1991.Genetics of *Caulobacter crescentus.* Methods Enzymol. **204:**372–384.
11. **Evinger, M., and N. Agabian.** 1977. Envelope-associated nucleoid from *Caulobacter crescentus* stalked and swarmer cells. J. Bacteriol. **132:**294–301.

12. **Garrett, E. S., D. Perlegas, and D. J. Wozniak.** 1999. Negative control of flagellum synthesis in *Pseudomonas aeruginosa* is modulated by the alternative sigma factor AlgT (AlgU). J. Bacteriol. **181:**7401–7404.
13. **Heydorn, A., B. K. Ersboll, M. Hentzer, M. R. Parsek, M. Givskov, and S. Molin.** 2000. Experimental reproducibility in flow-chamber biofilms. Microbiology **146:**2409–2415.
14. **Heydorn, A., A. T. Nielsen, M. Hentzer, C. Sternberg, M. Givskov, B. K. Ersboll, and S. Molin.** 2000. Quantification of biofilm structures by the novel computer program COMSTAT. Microbiology **146:**2395–2407.
15. **Janakiraman, R. S., and Y. V. Brun.** 1999. Cell cycle control of a holdfast attachment gene in *Caulobacter crescentus.* J. Bacteriol. **181:**1118–1125.
16. **Jensen, R. B., S. C. Wang, and L. Shapiro.** 2002. Dynamic localization of proteins and DNA during a bacterial cell cycle. Nat. Rev. Mol. Cell Biol. **3:**167–176.
17. **Kessler, B., V. de Lorenzo, and K. N. Timmis.** 1992. A general system to integrate *lacZ* fusions into the chromosomes of gram-negative eubacteria: regulation of the *Pm* promoter of the TOL plasmid studied with all controlling elements in monocopy. Mol. Gen. Genet. **233:**293–301.
18. **Klausen, M., A. Heydorn, P. Ragas, L. Lambertsen, A. Aaes-Jorgensen, S. Molin, and T. Tolker-Nielsen.** 2003. Biofilm formation by *Pseudomonas aeruginosa* wild type, flagella and type IV pili mutants. Mol. Microbiol. **48:**1511–1524.
19. **Koch, B., L. E. Jensen, and O. Nybroe.** 2001. A panel of Tn7-based vectors for insertion of the *gfp* marker gene or for delivery of cloned DNA into gram-negative bacteria at a neutral chromosomal site. J. Microbiol. Methods **45:**187–195.
20. **Lauriano, C. M., C. Ghosh, N. E. Correa, and K. E. Klose.** 2004. The sodium-driven flagellar motor controls exopolysaccharide expression in *Vibrio cholerae.* J. Bacteriol. **186:**4864–4874.
21. **Mattick, J. S.** 2002. Type IV pili and twitching motility. Annu. Rev. Microbiol. **56:**289–314.
22. **Nierman, W. C., T. V. Feldblyum, M. T. Laub, I. T. Paulsen, K. E. Nelson, J. A. Eisen, J. F. Heidelberg, M. R. Alley, N. Ohta, J. R. Maddock, I. Potocka, W. C. Nelson, A. Newton, C. Stephens, N. D. Phadke, B. Ely, R. T. DeBoy, R. J. Dodson, A. S. Durkin, M. L. Gwinn, D. H. Haft, J. F. Kolonay, J. Smit, M. B. Craven, H. Khouri, J. Shetty, K. Berry, T. Utterback, K. Tran, A. Wolf, J. Vamathevan, M. Ermolaeva, O. White, S. L. Salzberg, J. C. Venter, L. Shapiro, C. M. Fraser, and J. Eisen.** 2001. Complete genome sequence of *Caulobacter crescentus.* Proc. Natl. Acad. Sci. USA **98:**4136–4141.
23. **O'Toole, G. A., and R. Kolter.** 1998. Flagellar and twitching motility are necessary for *Pseudomonas aeruginosa* biofilm development. Mol. Microbiol. **30:**295–304.
24. **Poindexter, J. S.** 1964. Biological properties and classification of the *Caulobacter* group. Bacteriol. Rev. **28:**231–295.
25. **Prigent-Combaret, C., O. Vidal, C. Dorel, and P. Lejeune.** 1999. Abiotic surface sensing and biofilm-dependent regulation of gene expression in *Escherichia coli.* J. Bacteriol. **181:**5993–6002.
26. **Reisner, A., J. A. Haagensen, M. A. Schembri, E. L. Zechner, and S. Molin.** 2003. Development and maturation of *Escherichia coli* K-12 biofilms. Mol. Microbiol. **48:**933–946.
27. **Sambrook, J., E. F. Fritsch, and T. Maniatis.** 1989. Molecular cloning: a laboratory manual, 2nd ed. Cold Spring Harbor Laboratory Press, Cold Spring Harbor, N.Y.
28. **Simon, R., U. Priefer, and A. Pühler.** 1983. A broad host range mobilization system for in vivo genetic engineering: transposon mutagenesis in gram-negative bacteria. Bio/Technol. **1:**784–791.
29. **Skerker, J. M., and L. Shapiro.** 2000. Identification and cell cycle control of a novel pilus system in *Caulobacter crescentus.* EMBO J. **19:**3223–3234.
30. **Smit, J., C. S. Sherwood, and R. F. Turner.** 2000. Characterization of high density monolayers of the biofilm bacterium *Caulobacter crescentus*: evaluating prospects for developing immobilized cell bioreactors. Can. J. Microbiol. **46:**339–349.
31. **Smith, C. S., A. Hinz, D. Bodenmiller, D. E. Larson, and Y. V. Brun.** 2003. Identification of genes required for synthesis of the adhesive holdfast in *Caulobacter crescentus.* J. Bacteriol. **185:**1432–1442.
32. **Thormann, K. M., R. Saville, S. Shukla, D. A. Pelletier, and A. M. Spormann.** Initial phases of biofilm formation in *Shewanella oneidensis* MR1. J. Bacteriol. **186:**8096–8104.
33. **Tolker-Nielsen, T., U. C. Brinch, P. C. Ragas, J. B. Andersen, C. S. Jacobsen, and S. Molin.** 2000. Development and dynamics of *Pseudomonas* sp. biofilms. J. Bacteriol. **182:**6482–6489.
34. **Viollier, P. H., and L. Shapiro.** 2003. A lytic transglycosylase homologue, PleA, is required for the assembly of pili and the flagellum at the *Caulobacter crescentus* cell pole. Mol. Microbiol. **49:**331–345.
35. **Viollier, P. H., N. Sternheim, and L. Shapiro.** 2002. Identification of a localization factor for the polar positioning of bacterial structural and regulatory proteins. Proc. Natl. Acad. Sci. USA **99:**13831–13836.
36. **Wang, S. P., P. L. Sharma, P. V. Schoenlein, and B. Ely.** 1993. A histidine protein kinase is involved in polar organelle development in *Caulobacter crescentus.* Proc. Natl. Acad. Sci. USA **90:**630–634.
37. **Watnick, P. I., and R. Kolter.** 1999. Steps in the development of a *Vibrio cholerae* El Tor biofilm. Mol. Microbiol. **34:**586–595.
38. **West, L., D. Yang, and C. Stephens.** 2002. Use of the *Caulobacter crescentus* genome sequence to develop a method for systematic genetic mapping. J. Bacteriol. **184:**2155–2166.